SAR data for tropical forest disturbance alerts in French Guiana: Benefit over optical imagery

Marie Ballère, Alexandre Bouvet, Stéphane Mermoz, Thuy Le Toan, Thierry Koleck, Caroline Bedeau, Mathilde André, Elodie Forestier, Pierre-Louis Frison, Cédric Lardeux

Remote Sensing of Environment 252 (2021) 112159

Contents lists available at ScienceDirect

Remote Sensing of Environment

journal homepage: www.elsevier.com/locate/rse

SAR data for tropical forest disturbance alerts in French Guiana: Benefit over optical imagery

Marie Ballère [a,b,c,*], Alexandre Bouvet [d], Stéphane Mermoz [d,e], Thuy Le Toan [d], Thierry Koleck [a], Caroline Bedeau [f], Mathilde André [f], Elodie Forestier [f], Pierre-Louis Frison [c], Cédric Lardeux [g]

[a] Centre National d'Etudes Spatiales, 31400 Toulouse, France
[b] World Wildlife Fund France, 93310 Le Pré-Saint-Gervais, France
[c] LaSTIG, University of Gustave Eiffel, IGN, 77420 Champs-sur-Marne, France
[d] CESBIO, Université de Toulouse, CNES/CNRS/INRAE/IRD/UPS, 31400 Toulouse, France
[e] GlobEO, 31400 Toulouse, France
[f] Office National des Forêts Guyane, 97300 Cayenne, France
[g] ONF International, Paris, France

ARTICLE INFO

Keywords:
Near real time deforestation
Sentinel-1
Forest alert
Optical-SAR comparison
Tropical forest
French Guiana

ABSTRACT

French Guiana forests cover 8 million hectares. With 98% of emerged land covered by forests, French Guiana is the area with the highest proportion of forest cover in the world. These forests are home to an exceptionally rich and diverse wealth of biodiversity that is both vulnerable and under threat due to high levels of pressure from human activity. As part of the French territory, French Guiana benefits from determined and continuous national efforts in the preservation of biodiversity and the environmental functionalities of ecosystems. The loss and fragmentation of forest cover caused by gold mining (legal and illegal), smallholder agriculture and forest exploitation, are considered as small-scale disturbances, although representing strong effects to vulnerable natural habitats, landscapes, and local populations. To monitor forest management programs and combat illegal deforestation and forest opening near-real time alerts system based on remote sensing data are required. For this large territory under frequent cloud cover, Synthetic-Aperture Radar (SAR) data appear to be the best adapted. In this paper, a method for forest alerts in a near-real time context based on Sentinel-1 data over the whole of French Guiana (83,534 km2) was developed and evaluated. The assessment was conducted for 2 years between 2016 and 2018 and includes comparisons with reference data provided by French Guiana forest organizations and comparisons with the existing University of Maryland Global Land Analysis and Discovery Forest Alerts datasets based on Landsat data. The reference datasets include 1,867 plots covering 2,124.5 ha of gold mining, smallholder agriculture and forest exploitation. The validation results showed high user accuracies (96.2%) and producer accuracies (81.5%) for forest loss detection, with the latter much higher than for optical forest alerts (36.4%). The forest alerts maps were also compared in terms of detection timing, showing systematic temporal delays of up to one year in the optical method compared to the SAR method. These results highlight the benefits of SAR over optical imagery for forest alerts detection in French Guiana. Finally, the potential of the SAR method applied to tropical forests is discussed. The SAR-based map of this study is available on http://cesbiomass.net/.

1. Introduction

The Earth's tropical forests represent important biodiversity reserves and large carbon sinks for climate regulation. However, deforestation and forest degradation contribute greatly to biodiversity loss through habitat destruction (Whittle et al., 2012), soil erosion, terrestrial water cycle disturbances and anthropogenic CO2 emissions. Regarding the latter, deforestation and forest degradation accounted for 77% and 13%, respectively, of the total net flux attributable to land use and land cover changes over the period from 1850 to 2015 (estimated to have been 145 ± 16 PgC globally with 102 ± 5.8 PgC in the tropics, according to Houghton and Nassikas (2017)).

The detection of annual forest disturbance surfaces is useful for many applications, such as estimating CO2 emissions (Friedlingstein et al.,

* Corresponding author at: 18 avenue Edouard Belin, 31400 Toulouse, France.
E-mail address: marie.ballere@cnes.fr (M. Ballère).

https://doi.org/10.1016/j.rse.2020.112159
Received 23 January 2020; Received in revised form 19 October 2020; Accepted 21 October 2020
Available online 5 November 2020

2019). It is also used by international programs for forest conservation, such as Reducing Emissions from Deforestation and Forest Degradation (REDD+) and the Role of Conservation, Sustainable Management of Forests and Enhancement of Forest Carbon Stocks in Developing Countries. Forest loss at the annual scale has been monitored using Earth observation satellites, and some of the resulting maps are provided openly (Hansen et al., 2013; Valeriano et al., 2004).

Forest Alert (FA) systems complement these annual observations with more frequent forest monitoring. While these systems play a valuable role in prioritizing resources allocation for law enforcement and conservation, most Early Warning Systems are not designed to quantify the amount of change for in-depth reporting or analyses.

Several research and government organizations have developed systems that provide regular updates to the public, principally based on optical remote sensing data. With a coarse spatial resolution (MODIS data, 250 m), the FORMA (Wheeler et al., 2014), Terra-I (Reymondin et al., 2012) and IDEAM systems are developed at the pantropical scale (except IDEAM covering only Colombia) and are respectively available biweekly, monthly and quarterly. DETER-B (Diniz et al., 2015), a Brazilian operational system, provides results with a 60-m spatial resolution and a 5-day frequency. It is developed by the Instituto Nacional de Pesquisas Espaciais (INPE), based on AWiFS data and including a photointerpretation step. Finally, with the medium resolution of 30-m Landsat data, the MINAM (Peru) and the University of Maryland (UMD) produce FA datasets every week: PNCB Early Warning Alerts and Global Land Analysis and Discovery (GLAD) FA (Hansen et al., 2016).

Such operational FA systems should allow states or forest managers to fight against drivers of deforestation, which are generally linked to illegal activities. They can also be used for protected areas management, community forest monitoring, management of agricultural and other productive concessions and raising awareness. A Near-Real Time (NRT) deforestation-monitoring protocol starts with forest losses detection as precisely and quickly as possible (Finer et al., 2018). Such methods require detection with high accuracy and high temporal and spatial resolution, especially for sites containing small-scale deforested patches. Globally, the detection of large areas (>3 ha) is now well controlled (Kalamandeen et al., 2018) and efforts should be concentrated on areas of smaller density and size as their number increases.

French Guiana is located in South America, and it is mainly affected by small-scale deforestation (Alvarez-Berríos and Mitchell Aide, 2015) and has a low deforestation density. With primary Amazonian forest covering more than 95% of its territory (Keenan et al., 2015), French Guiana has unique natural resources but is not exempt of threats. Gold mining is the main cause of these deforestation: Rahm et al. (2017) reported more than 25,000 ha affected until 2015. The resulting pollution of the river has led to health issues due to the use of mercury and the increase in turbulence and turbidity, which have degraded biodiversity, thus highlighting the need of early detection system for forest disturbance.

One would expect using the GLAD FA to monitor this large area because it is fully automated based on free data and therefore cost efficient; however, the persistent cloud cover limited its use, as does, in a lesser extent, the Landsat resolution.

A specific alert system dedicated to illegal gold mining has been operational since 2006 (Linarès et al., 2008) and is based on the photointerpretation of optical imagery (Landsat at first, then SPOT-5 up to 2015, and Pleiades and Sentinel-2 currently) to detect patches of deforestation and water turbidity. This system performs better than the GLAD FA as it uses higher resolution imagery, specific knowledge of the analyst and each alert is verified by an airborne mission after its detection. However, such a system is equivalent to a high cost.

Moreover, those products based on optical data are principally limited by the cloud cover that is persistent in the tropics. During wet seasons the cloud cover may cause important temporal detection delays, which contradicts the need for fast deforestation alerts.

Cloud cover free Synthetic-Aperture Radar (SAR) images have great potential in tropical areas, allowing to build operational Forest Alerts system but have rarely been used for deforestation monitoring compared to optical imagery (despite multiple research works, see Lardeux et al. (2019); Mermoz and Le Toan (2016); Lohberger et al. (2018); Reiche et al. (2018)), partly because of the scarce data availability (Reiche et al., 2016) until the Sentinel-1 program. An exception is the JJ FAST system developed by the JAXA/JICA, based on ALOS-2 radar data that produce FA on 77 tropical countries every 1.5 months and with a spatial resolution of 5 ha (Watanabe et al., 2017).

Since the launch of the Sentinel-1, SAR images are now easily accessible at the global scale, with systematic acquisitions at a 5×20-m spatial resolution and a 6- to 12-day revisit time (depending on the location) in all weather conditions. The continuity of the program is also ensured until at least 2030. However, the C-band frequency of the Sentinel-1 SAR system is less adapted for forest/deforested area detection than the longer wavelengths because it may lead to confusion between the forest canopy and deforested area. This is caused by the backscatter variability of deforested area having a diversity of surface conditions (surface roughness, soil moisture content, and the remnant vegetation and debris). Recently, it was demonstrated that deforestation can be detected using Sentinel-1 dense time series based on a reliable indicator that bypasses environmental effects on SAR signals (Bouvet et al., 2018). Despite the research results using SAR data for forest loss alerts in the tropics, no evaluation at a country scale has been done yet.

In this study, we develop a forest loss alert system over a country-scale territory, namely, French Guiana, based on the method developed by Bouvet et al. (2018) using Sentinel-1 SAR data (subsequently called FA1). French Guiana, concerned by gold mining, forest exploitation and agriculture offer a large panel of logging practices: small to large areas, legal and illegal activities, logging during the dry season or the whole year and various methods of logging (clearcutting, slashing and burning, etc.). The detection results are assessed using reference ground data, and are compared with the GLAD Forest Alerts (subsequently called FA2).

As a first step, FA1 is computed over the whole of French Guiana from 2016 to 2018 in a NRT context to raise awareness to new forest loss every 6 days with a minimum mapping unit (MMU) of 0.2 ha. The validation is processed using a high-quality reference dataset from French public organizations, used operationally as a reference for gold mining monitoring and forest exploitation management. We used a probability-based stratified random sampling protocol on the 3 types of deforestation. The results are first evaluated in terms of sensitivity of the approaches to the different spatial patterns encountered for the 3 deforestation types. In the second step, we evaluated the potential of the methods for NRT monitoring. Then, we analyze the deforested parcel size and the annual forest loss from 2016 to 2018 calculated with FA1 over the whole French Guiana, in comparison with FA2 and also with the GFW-measured annual tree cover loss. Finally, we discuss the operational use of FA1.

The study area, the data and methods of validation and comparison are described in Section 2 of this paper. Section 3 presents the results and highlights the difference between the SAR FA method and the optical FA method. Finally, a discussion is provided in Section 4, and conclusions are given in Section 5.

2. Material and methods

2.1. Study area

French Guiana is a French territory located in northern South America near the equator and spans 83,534 km^2, with approximately 95% of its land mass covered by primary forest. In terms of climate, French Guiana has a tropical rainforest climate characterized by a long wet season from December to June (rainfall from 250 to 550 mm per month) and a dry season from July to November (100 to 180 mm of rainfall per month). Note that a short dry season (the short summer of

March) sometimes occurs for one and a half months, with less rainfall (170 to 370 mm per month) than during the wet season. The annual mean cloud cover in French Guiana is 67%.

As stated in the previous section, the main drivers of deforestation and canopy opening in French Guiana are gold mining (legal and illegal), smallholder agriculture and forest exploitation.

2.1.1. Smallholder agriculture

Smallholder agriculture for subsistence farming (Fig. 1) is the prevalent driver of deforestation related to agriculture. Smallholder agriculture is based on slash-and-burn practices characterized by the cutting and burning of small areas (ranging from 0.2 to 1 ha in size) only between July and November (during the dry season). Each parcel is exploited (and so slashed-and-burned before planting) for 2–3 years before a fallow period. The French policy of monitoring the land registry and allocating land for agriculture, is currently encouraging agricultural development for profit (Demaze and Manusset, 2008). With population growth, the demand for agricultural land increases along with forest loss. Nevertheless, slashing is still mainly a practice of subsistence agriculture and does not cause significant environmental effects.

2.1.2. Forest exploitation

Forest management for wood exploitation is well regulated by the French Office National des Forêts (ONF) (Fig. 2). Reduced-impact logging practices are implemented: removal of only 25 m3 of wood per ha (4 to 5 trees) is allowed, and parcels can be exploited only once every 65 years (Office National des Forêts, 2019). Tree cutting and skid-trail creation occurs year round but represents small area changes that are not expected to be detected with precision. The largest extent of canopy opening due to forest exploitation is related to building roads and depends on the type of road, main road axes or secondary roads. Landings (of 0.1 to 0.5 ha) and log yards (up to 1 ha) are created on roadsides to store the wood. Roads, log yards and landings are generally created during the dry season (from July to December), although some steps in landing creation take place during the wet season (understory clearing and sometimes tree cutting).

2.1.3. Gold mining

The majority of gold mining (Fig. 3) in French Guiana occurs year round and is mainly alluvial. Legal mining operations are often operated by large companies and span over large creek areas. French law forces companies to restore the exploited area and forbids the use of mercury. Since illegal operations are usually smaller than large-company operations, the exploited areas can be found in steep valleys. Illegal practices are investigated by the French Army, which makes gold miners often move away and exploit the same area several times. The line between legal and illegal is tenuous, and illegal practices are also found in legal projects. In illegal operations, mercury and cyanide are used to extract gold, which are then released in rivers. Gold mining produces a large environmental impact, leading to sanitary and health issues (Miller et al. (2003); De Kom et al. (1998); Eisler (2004)). The increase in sediments released in rivers leads to biodiversity loss. Gold miners working near the local population bring insecurity, loss of culture and social conflicts (WWF (2018); Forte (1999); Colchester (1997)). Moreover, poor living conditions in mining camps (e.g., prostitution) contribute to the spread of diseases (e.g., HIV, malaria) (Palmer, 2002). Detection of illegal gold mining is therefore of environment and social importance for French Guiana.

2.2. Data

2.2.1. Sentinel-1 data

We used Sentinel-1 images with a 250 km width acquired over French Guiana in interferometric wide (IW) swath mode from 8 November 2015 to 31 December 2018. Ground Range Detected (GRD) products, characterized by a resampling at a 5 × 20-m spatial resolution cell to obtain a 10 × 10-m pixel size, were used. French Guiana is covered by 7 Sentinel-1 images, and a total of 1639 images were acquired and used over the study period.

Over the study area, Sentinel-1A provides consistent time series from 8 November 2015 with a 12-day revisit time in the ascending and descending passes. Since 26 September 2016, the revisit time has been reduced in the ascending path from 12 to 6 days, with the data acquisition of 2 satellites, i.e., Sentinel-1A and 1B. Preprocessing was performed by S1 Tiling (Koleck et al., 2019), an automated chain that handles images downloading, calibration in γ_0, orthorectification and spatial and temporal filtering (Quegan and Yu (2001) on a 3 × 3 window size and adapted to a NRT context, see Section 2.3.1).

2.2.2. Reference data for validation

We used various sources of reference data addressing different drivers of deforestation, all coming from French organizations and used as a reference for the French Guiana forest monitoring. All deforestation-related data available for 2017 and 2018 and over plots larger than 0.2 ha were used (Table 1).

Smallholder agriculture reference data are annually produced by the Parc Amazonien de Guyane (PAG). Polygons are detected by photointerpretation of SPOT, Pleiades, Landsat or Sentinel-2 data and most of them were checked in the field. Over a 423,585 ha zones (Fig. 4, in orange), 665 polygons were new forest loss: labelled “old forest” until 2016 (included) and “slashed-and-burned” in 2017 or 2018. After applying the MMU of 0.2 ha, there are 602 polygons remaining, totaling 285.7 ha of slashed-and-burned patches (0.067% of the 423,585 ha area). The reference date is the year when clearcutting of the parcel was implemented.

Reference data of newly built roads, log yards and landings for forest

Fig. 1. Photos of a smallholder agriculture parcel slashed: trees are still on the ground and vegetation is drying out (left) and photos of a smallholder agriculture parcel burned: only trunks are left on the ground (right). Copyright: Marie Ballère.

Fig. 2. Photos of roads (left) and log yards (right) built for forest exploitation. In both cases, forest has been replaced by bare soil and there is nothing on the ground except log. The ground is smooth in most cases but can be rough with the activity of machines. Copyright: ONF.

Fig. 3. Aerial photograph of legal gold mining operations: the area is large and composed by water basins and bare soil (left). Aerial photograph of illegal gold mining operations: only a small surface of forest has been removed (right). Copyright: ONF. (For interpretation of the references to colour in this figure legend, the reader is referred to the web version of this article.)

Table 1
Number and sizes of the reference polygons for the various types of deforestation in French Guiana.

	Number of areas	Mean size (ha)	Std size (ha)	Total surface (ha)
Smallholder agriculture	602	0.47	0.35	285.7
Forest exploitation	82	1.31	3.61	107.8
Gold mining	1183	1.46	2.1	1731

exploitation acquired in situ and then digitized have been made available by the ONF. Roads were in a line shapefile, and we applied a 20-m buffer zone (actual size). Over a 26,630 ha zone (Fig. 4, in green), 82 polygons were selected, totaling 107.8 ha of canopy opening due to forest exploitation (0.40%). The reference date of the log yards consists of a range of dates for the optical-based observations before and after the disturbance event, including 30% dated by the month. Over roads, the reference date is the year of disturbance

Gold mining data are continuously collected by the Observatoire de l'Activité Minière (OAM, Mining Activity Observatory) and managed by the Etat-Major de l'Orpaillage et de la Pêche Illicite (EMOPI). In particular, the ONF provides spatialized information based on photo-interpretation of SPOT, Pleiades, Landsat or Sentinel-2 images and these data are systematically verified by aerial surveys. In 2017–2018, 1183 polygons were digitized. These polygons are spread over a 5.8 Mha zone (Fig. 4, in yellow), totaling 1,731.0 ha of disturbances (0.03%). The reference date associated with each gold mining patch is the date of the first observation using optical images.

The reference dataset presented above is accurate enough for operational use because expert analysts use various images sources, including high-resolution imagery up to 2.8 m with Pleiades for photo-interpretation, and digitalized polygons are checked in the field afterward.

However, these data have been used for the creation of strata for spatial validation only, in order to reduce geolocation and omission bias. Note that the reference datasets do not contain accurate deforestation dates because such information could not be obtained over this large territory.

2.2.3. *Dataset for comparisons (FA2)*

GLAD FA (Hansen et al., 2016) is a deforestation alert product generated weekly, which we consider NRT in this paper. This product provided by the GLAD laboratory at UMD, is free and available at a large scale (from 30 degrees north to 30 degrees south, in addition to Russia's Far East). It is based on Landsat (optical) images with a 30-m resolution.

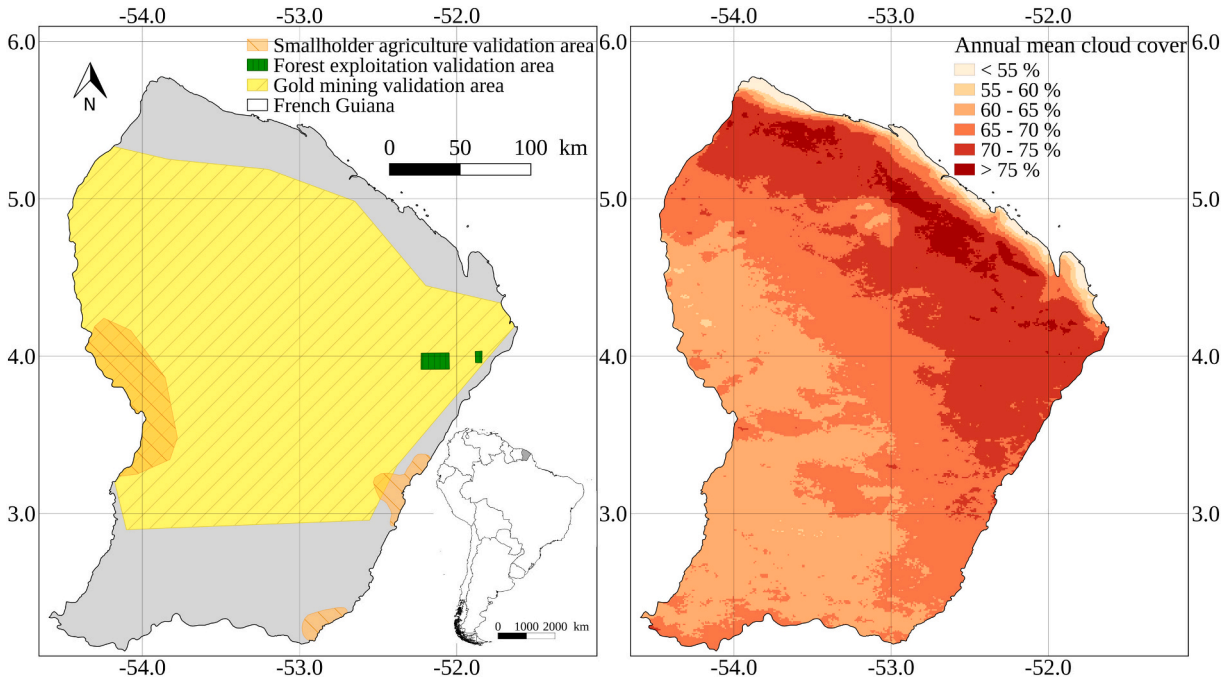

Fig. 4. Left: French Guiana with the validation areas for each type of deforestation (orange: smallholder agriculture, green: forest exploitation, yellow: gold mining); Right: Annual mean cloud cover of French Guiana. (For interpretation of the references to colour in this figure legend, the reader is referred to the web version of this article.)

An alert is raised when a 50% of a pixel's canopy cover is lost. The alert is then confirmed if at least 2 of 4 consecutive exploitable Landsat products for a period of 180 days show canopy loss. The persistent cloud cover over tropical areas is thus a significant limitation of the NRT deforestation detection method because few images are usable. This alerting system is meant to complement current annual global forest cover loss products. In other words, the alert system does not provide area estimates (Hansen et al., 2016) but provides the date of the first observation of deforestation. The deforestation is then confirmed after 16 to 180 days.

The GFW Tree Cover Loss Map is an annual map of forest cover loss (Hansen et al., 2013). It is also produced by the UMD at a 30-m resolution. The map shows the total deforestation area in a year.

2.2.4. Forest/non-forest map

Forest/non-forest maps are necessary to filter changes detected only on forests and to remove false alarms due to changes in other land use-land cover classes (agriculture, bare land, water, etc.). The forest/non-forest map used in this study was produced by (Rahm and Lardeux, 2019) with 2015 data to form a mask for the beginning of the study in 2016. Various data coming from land cover maps of the ONF and the PAG were aggregated and homogenized to create the non-forest class. It also integrates non-forest polygons from the photointerpretation of 2015's optical images in areas not covered by previous land cover maps.

2.3. Methods

2.3.1. Deforestation alert algorithm (FA1)

Traditional methods of deforestation detection are established on the hypothesis that SAR backscattering decreases when disturbances occur. However, at C-band, the backscattering does not necessarily decrease because rainfall and/or trees remaining on the ground, for example, leading to high backscatter values. To solve this problem, FA1 based on Bouvet et al. (2018) use the detection of SAR shadowing in the SAR time series. Shadowing occurs in SAR images because of the particular side-looking viewing geometry of SAR systems. A shadow in a SAR image is an area that cannot be reached by any radar pulse. Shadows created by trees at the borders between forest and non-forest areas can be observed in high-resolution SAR images, depending on the viewing direction. The shadows that appear after deforestation are characterized by a sudden backscatter drop in the SAR time series. Due to the purely geometrical nature of the shadowing effects, this decrease in backscattering is expected to persist over time and false alarms must be avoided. New shadows should consequently remain visible for a long time and are easily detectable when dense SAR time series data, such as Sentinel-1 time series data, are available. Forest loss is detected using the radar change ratio (RCR; Tanase et al., 2018), which is the ratio of the post-disturbance- to predisturbance-averaged backscattering (Eq. 1).

In a time series of N dates, the backscatter change in a given pixel at date d_i ($i \in (1,N)$), denoted by γ^0_i, that occurs between date d_i and date d_{i+1}, is measured by the following RCR:

$$RCR_i = M_a / M_b \tag{1}$$

where M_b (Eq. 2) is the mean backscatter value in X_b available images until date d_i (inclusive), and M_a (Eq. 3) is the mean backscatter value in the X_a images acquired after date d_{i+1} (inclusive):

$$M_b = \frac{1}{X_b} \sum_{j=i-X_b+1}^{i} \gamma_j^0 \tag{2}$$

and

$$M_a = \frac{1}{X_a} \sum_{j=i+1}^{i+X_a} \gamma_j^0 \tag{3}$$

In this study, we use all the available images before date d_i for the calculation of M_b, and X_a is set to 3, which represents a tradeoff value between speckle filtering on one hand and timely provision of results on the other hand. The RCR is used for the first time to detect newly appeared shadows by applying a threshold of −4.5 dB on the image formed by the temporal minimum RCR value calculated over a given period. The extent of the deforestation area is subsequently reconstructed by using a less drastic threshold (−3 dB) to the same minimum RCR image on the pixels neighboring the detected shadows to detect

potentially deforested pixels. An MMU is applied afterwards.

SAR signal is affected by topography and 12% of French Guiana has a slope higher than 15°. With this method, the slope has a low impact on the detection, because the approach is based on thresholds applied on the backscatter change and not directly on the absolute backscatter value. However, on steep slopes a pixel may be saturated and return an inconsistent signal. To avoid false alarms in the shadow detection step, the shadows detected in areas with slopes higher than 15° are removed. Once the deforestation is confirmed by the presence of a shadow, the threshold on slope is not applied for the second step (detection of the pixels neighboring the detected shadow to reconstruct the whole deforested surface), because it could remove the middle of a deforested area spanning over a slope. Finally, having the ascending and descending orbits allow two views of a pixel. A pixel located in a radar shadow (on the backscatter image, not in the change image) in an orbit direction, will be visible in the other orbit direction.

In this study, the method was applied over the whole of French Guiana. The studied time period is 3 years. To use this method on such a long time series, choices for information retention time, i.e., the duration of the period over which the temporal minimum RCR values are calculated, have to be made. This period must be long enough so that areas progressively cut over several weeks can reach a sufficient size with respect to the MMU. However, the period must not be too long: isolated pixels wrongly detected as shadows because of the remaining speckle noise could accumulate and reach a size sufficient to be considered a shadow. We chose here a 6 month sliding window and an MMU of 0.2 ha, which both empirically appear to be good tradeoffs between ground observations and avoidance of false alarms.

2.3.2. Spatial validation method

The objective is to evaluate the accuracy of the detection of forest loss and intact-forest produced by FA1. In order to assess the sensitivity of the method to different spatial patterns, we performed separately the evaluation for 3 deforestation types (smallholder agriculture, forest exploitation and gold mining). Note that for comparison purposes, FA2 was assessed with the same method and we performed the validation on 2017 and 2018 only, due to FA2's availability.

For the spatial evaluation, we used a probability-based stratified random sampling protocol (Olofsson et al., 2014) facilitating sufficient statistical representation of each class of the map in this low deforestation context.

The stratification is a partitioning of the Regions Of Interest (ROI) in which each assessment unit is assigned to a single stratum. One most common attribute used to construct strata is the classes determined from the map (deforested area and intact forest in our case). The purpose of this stratification is to improve the precision of class-specific accuracy. The strata "deforested area" was formed by the reference data collected from French organization (see section 2.2.2). The strata "intact-forest" were remaining areas of the ROI. Non-forest areas were masked a priori using the forest/non-forest map described in section 2.2.4. A random sample selection was performed within each stratum. The sample size formula of Cochran (1977) - eq. 5.25) suggests a sample size of approximately 900 assessment units, although assessing separately 3 types of deforestation, we would have had 2,700 samples in total and that would have been too time-consuming. Moreover, the global evaluation would have been based on 2,700 samples (instead of 900 suggested). As a trade-off and an acceptable time cost, we used 500 samples per type of deforestation (for a total of 1,500 samples). The sample units were allocated following the recommendations in Olofsson et al. (2014, 2020) such that 50 were selected in the deforestation stratum and 450 samples in the "intact-forest" stratum. This represents 500 samples per type of deforestation, and a total of 1,500 samples considering all 3.

A point with a 10-m buffer is used as a spatial assessment unit. The labelling of the selected samples was generated by visual interpretation of optical imagery time-series (using the Sentinel Hub EO Browser and Google Earth). A sample is considered to be mapped by a class if its surface is in majority covered by pixels of this class. Out of the total 1,500 interpreted samples randomly generated, 1,487 samples were retained: 5 intact forest points were removed and 5 were finally classed as deforested. Nine deforested points were already deforested at the beginning of the study or not deforested at the end of the study and were thus removed. Finally, 4 points were removed as it was impossible to interpret them due to the lack of cloud-free data.

Following the good practices recommendations from Olofsson et al. (2014), the error matrix should be reported in terms of estimated area proportion rather than in terms of sample counts using the Eq. (4) of Olofsson et al. (2014). Using this unbiased estimator would allow for the computation of error-adjusted area estimates and their uncertainties. However, as mentioned in Olofsson et al. (2020), the effects of omission errors are exacerbated in a situation where the area of forest change is low relative to the area of intact forest. In French Guiana, the proportion of forest change is extremely low (about 0.07% relative to intact forest) and using estimated area proportion for accuracy assessment would therefore not be adapted. As the effects of the omission are reduced with the forest stratum weight, the recommendation from Olofsson et al. (2020) is to split the forest stratum into a small substratum that contains all the omission errors and a large substratum that is free of omission errors. To achieve this, an approach exemplified in the remote sensing literature is the use of a buffer strata to mitigate the effects of omission errors (Arévalo et al. (2020); Bullock et al. (2020); Potapov et al. (2017); Tyukavina et al. (2013)). This solution is based on the hypothesis that change mostly occurs in clusters and therefore omissions of change typically occur close to areas of mapped change while areas mapped as stable forest at larger distances from mapped change are unlikely to contain omissions. However, the buffer size shall remain relatively small in order to keep its efficiency in the reduction of the weight of omission errors. French Guiana has low-density deforestation. Deforestation due to gold mining can be more than 10 km away from any other deforestation. Therefore, the inclusion of all omission errors in a buffer stratum would require a very large stratum, which would lead to poor efficiency. The buffer approach is therefore not indicated in the case of low-density deforestation. Because of the specific situation in French Guiana (extremely large area of intact forest relative to area of forest change and low-density deforestation), we decided to report the accuracies based on sample counts.

2.3.3. Temporal comparison method

The dates of forest loss associated with the reference data were not accurate enough for a reliable temporal validation of FA1 estimated detection dates (cf. section 2.2.2). Moreover, the difficulty in visually interpreting SAR images and the low recurrence of exploitable optical images did not permit to build a reliable temporal validation dataset and therefore compute a real temporal uncertainty. In order to evaluate the potential of the methods for NRT monitoring, we compared the estimated dates from FA1 and FA2 in 2017 and 2018 as the spatial validation. To do so, we computed for both FAs the median values of the detection dates of all the pixels contained over each reference polygon. As long as a part of a FA dataset intersects a reference data polygon, the latter is considered detected by the FA. Note that for the temporal comparison, we kept only reference data polygons detected by both methods, which represents 41.6% of the total amount of reference data.

In French Guiana, Sentinel-1 provides an exploitable image every 6 days in the ascending pass, and 12 days in the descending pass. Therefore, a deforestation will occur at a maximum of ±3 days of a Sentinel-1 exploitable image and the whole territory is viewed 3 times every 12 days. With Sentinel-1's revisit time, the FA1-confirmed alert delay is 12 days.

Regarding the Landsat time resolution of 16 days, a deforestation will occur at a maximum of ±8 days from an acquisition, although in practice, observation availability is limited by the Landsat acquisition strategies and cloud cover. The maximum delay between a deforestation and its observation through Landsat is then variable as well as the alert

confirmation delay.

3. Results

On the whole (Table 2), FA1 validation results show high user's accuracies (>91%) for all deforestation types and intact forest, and producer's accuracies higher than 75.4%. FA1 overall accuracies are 97.8% on average and generally 4% higher than FA2's overall accuracies. The noticeable difference concerns the producer's accuracies of the deforested class: FA1 scores are 38.9% to 57.1% higher than FA2 depending on the deforestation type, meaning that FA1 produces less omission errors (i.e., detects more effective deforestation).

However, FA2 shows 100% of user's accuracies for all the deforested class, expect for forest exploitation (95.2%). Those performances are on average 2.1% higher than FA1, which means that FA2 produces less commission errors on deforestation (more confidence in an effective detection).

3.1. Spatial validation of the produced SAR dataset: FA1

FA1 shows high performance (Table 2) with a global producer's accuracy of 81.5% for the deforested class and 99.6% for the intact forest. Global user's accuracies are 96% and 98% (respectively). The global overall accuracy of FA1 is 97.8%.

The smallholder agriculture, i.e., small, slashed-and-burned parcels of 0.47 ± 0.35 ha (see Table 1) is the type of deforestation reaching the highest producer's accuracy: 89.4%. Such single events lead to shadow detection in one piece, and the weather condition (dry season) is optimal to see a decrease in the whole parcel area, with few rainfalls that can affect the SAR signal. Moreover, burning often leads to a decrease of backscatter with less vegetation remaining on the ground.

For forest exploitation, the producer's accuracy is 75.9%. One-third of the omissions were on rectangular-shaped landings on an existing road side. The other two-thirds are on roads, i.e., long and thin (~20 m) objects. This type of shape is at the limit of what can be done with a sensor resolution of 20 m. Note that a larger shadow will appear on a road built parallel to the orbit trajectory. Therefore, new north-south roads are better detected than west-east road because of the orbit track. Of the total road surface area from the reference data, 43% was detected.

Gold mining reaches an 80% producer's accuracy. Gold mining sites can be small or large (1.46 ± 2.1 ha, see Table 1) and often have a meandering shape (and, more rarely, a circular shape) because they follow rivers. The few omission errors were found on meandering shapes, particularly when they are thin (~20 m), similar to the roads.

The producer's and user's accuracies for intact forests are higher than 97% in all cases, meaning that the intact forests are not overestimated.

Fig. 5 shows two maps of the forest disturbance detection results due to smallholder agriculture (left) and gold mining (right). It is interesting to observe the gradual temporal evolution of the gold mining areas compared to singles slash-and-burn events in smallholder agriculture.

Table 2
Validation of the FA1 (SAR) and FA2 (optical). UA means User's accuracy and PA means Producer's accuracy.

	Smallholder agriculture		Forest exploitation		Gold mining		Global (3 types of deforestation combined)	
	FA1	FA2	FA1	FA2	FA1	FA2	FA1	FA2
UA deforested area	97.7	100	91.1	95.2	100	100	96.0	98.1
UA intact forest	98.9	93.3	97.1	92.9	98.0	94.3	98.0	93.5
PA deforested area	89.4	31.9	75.9	37.0	80.0	40.0	81.5	36.6
PA intact forest	99.8	100	99.0	99.7	100	100	99.6	99.9
Overall accuracy	98.8	93.5	96.5	93.0	98.2	94.6	97.8	93.7

3.2. Spatial comparison to the optical dataset: FA2

FA1 detected more deforestation than FA2 because we could explain by the resolution of each sensor and the low sensitivity of Sentinel-1 to cloud cover.

The global overall accuracy of FA2 is 93.7%. The advantage of FA2 is that it makes very few commission errors, although it produces significantly fewer forest alerts than FA1: the global producer's accuracy of deforested areas is 36.3%.

For smallholder agriculture, FA2 found 31.9% of the deforested area (Table 2). The smallholder agriculture practice almost only occurs during the dry season, which allows for a comparison under cloud-free conditions. However, this deforestation type shows the maximum gap between FA1 and FA2 producer's accuracy. Indeed, Sentinel-1's higher resolution is better suited to detect small plots as smallholder agriculture (see Table 1).

The validations for forest exploitation and gold mining show the same trends with 37.0% and 40.0% producer's accuracy values, respectively, for deforestation. The FA2 omission errors for forest exploitation were equally distributed over roads and log yards/landings. For gold mining, two-thirds of the omissions were on samples with small surface areas or long, thin shapes. The other third was on a large meandering-shaped surface area, and the sample was missed because of poor detection of the area overlapping the real deforested surface area (Fig. 6). On large, legal gold mining sites, forest replacement by bare soil and water can remain visible for multiple years. Regarding those sites, half of the deforested samples correctly classified by FA1 and missed by FA2 occurred in the wet season, and half occurred in the dry season. This finding shows that beyond temporal delays, persistent cloud cover makes finding two exploitable images in a 180-day window very difficult at some sites.

Most of the time, the shape of the deforestation is less accurate in FA2, and some areas are missing, as shown in Fig. 6.

To illustrate and evaluate this phenomenon, Fig. 7 shows the histogram of the percentage of the surface area of each reference polygon detected by each method. Among the reference polygons detected by each approach, FA1 tends to delineate more completely the disturbed areas with respect to FA2.

In total, FA1 and FA2 detections intersected 1,339 and 867 reference polygons respectively. 783 reference polygons were detected by both FA1 and FA2. This means that 84 reference polygons were only intersected by FA2 detections and 556 only by FA1, which shows the complementarity between both detection methods.

To conclude, FA2 misses more disturbed areas (PA < 40%) than FA1 and therefore overestimates intact forest compared to FA1 (PA > 75%), regardless of the type of deforestation. This finding can be explained by the fact that alerts raised by FA2 might have been detected and then were not confirmed because of persistent cloud cover (>180 days). In addition, FA2 is based on 30-m resolution Landsat imagery, whereas FA1 is based on 10-m resolution Sentinel-1 imagery. Note that this analysis concerns relatively small plots of deforestation compared to those found in very dynamic landscapes with high deforestation rates. Therefore, FA2 spatial results may not be representative for large forest clearing and the spatial advantage of FA1 over FA2 could be reduced in this case.

3.3. Temporal comparison between the SAR dataset (FA1) and the optical dataset (FA2)

We performed a comparison of the detection dates estimated from FA1 and FA2 directly. The objective is to determine which approach detects closest to the true deforestation date. The rationale is that there

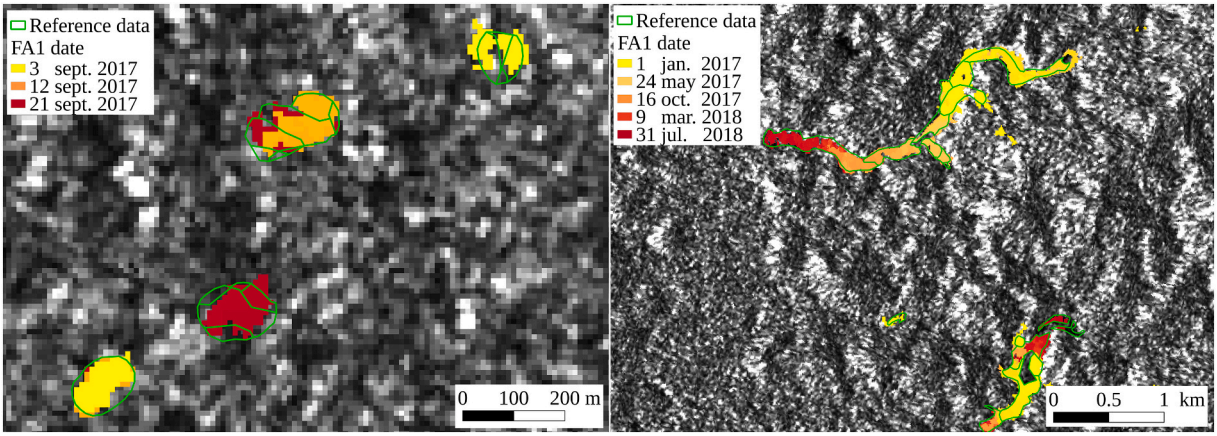

Fig. 5. FA1 maps of the forest disturbances detection results due to slash-and-burn (left) and gold mining (right). Colors shows the alert date detected by the algorithm. Green lines are the borders of reference polygons. The left map is centered on 3°40 N and 54°3 W. Background: Sentinel-1 SAR image. (For interpretation of the references to colour in this figure legend, the reader is referred to the web version of this article.)

are well-known causes that can lead to delayed detections (e.g., cloud cover for optical data, remaining vegetation for SAR data) but no identified cause that can lead to anticipated detections (before the actual occurrence of deforestation). Therefore, when FA1 and FA2 provide different deforestation dates, the earlier detection is considered to be closer to the true forest loss date than the later detection. In the following, only the reference polygons detected by both methods are used for the temporal comparison.

3.3.1. Smallholder agriculture

Regarding smallholder agriculture, 410 polygons were detected by FA1, 243 polygons were detected by FA2 and 210 polygons were jointly detected by the two methods.

In Fig. 8, the left panel represents the number of polygons detected monthly (green for FA1 and yellow for FA2). Both algorithms detect deforestation during the dry season (July to November), as expected, when slash-and-burn agriculture happens. During the dry season, the cloud cover is reduced, as is the temporal delay between FA1 and FA2.

The right panel of Fig. 8 shows that the differences in the dates between FA1 and FA2 are generally distributed around zero (mean of 20 days earlier for FA1, standard deviation = 121 days). The positive part shows polygons first detected by FA2, and vice versa.

In approximately 50% of the cases, the date difference between the two methods is smaller than the revisit period of Sentinel-1 (12 days) or Landsat (16 days) and may therefore be explained by the timing of the acquisitions (Fig. 8, in orange) of each sensor with respect to the considered forest loss event, rather than by intrinsic limitations of each sensor.

Smallholder agriculture parcels found by FA1 approximately one year before (10%) are first logged in the 2017 dry season and are detected by FA2 only in the 2018 dry season during the second clear-cutting event of the parcel. Polygons detected approximately 200 days before by FA1 correspond to a detection delay due to cloud cover: logged at the end of 2017 and detected by FA2 during the short summer of 2018.

Surprisingly, some polygons were found much earlier by FA2 (more than 3 months) than by FA1. The analysis of these polygons shows that the delays correspond to errors when allocating the deforestation date with FA2. This phenomenon happens when a parcel logged in 2018 is not detected by FA2 but is intersected by a neighboring parcel correctly detected in 2017, as illustrated in Fig. 9. It creates a 1-year error in the delay analysis (Fig. 8, in red).

In the end, FA1 detects more polygons in advance of FA2, although the temporal difference between the two algorithms is not significant for smallholder agriculture, which leads to confidence about the logging date estimation provided by both methods in this case.

3.3.2. Forest exploitation

On forest exploitation, 51 polygons were detected by FA1 and 32 by FA2. Twenty-eight polygons were jointly detected by the two methods, and most of them were linked to disturbances that occurred in 2017 when more reference data were available. Most alerts are raised during the dry season and the short summer (Fig. 10), which is when most of the activities that create a large opening in the canopy happen.

More than 90% of the disturbed areas are first detected by FA1 (Fig. 10).

The delay can be explained by the timing of acquisitions for only two samples. For all the other samples, the delay is attributable to the method and to the sensor. Regina/Saint-Georges forest (the location of this exploitation study site) is among the cloudiest areas in French Guiana (the mean cloud cover is >65%, see Fig. 4), explaining why the delay in optical detections is more important in this study site than in the smallholder agriculture site.

3.3.3. Gold mining

Regarding gold mining, 878 polygons were detected by FA1, and 592 polygons were detected by FA2. 545 reference polygons were jointly detected by both methods. Gold mining activities remained sustained all year round, even if there were variations. Illegal gold mining is dependent on the water level for river freight, and it is impossible to run the pumps for alluvial mining without water. However, heavy rains from April to June can cause heavy leaching and drown the sites as the water level rises.

For legal gold mining, the start of exploitation is easier in the dry season, although their equipment allows them to work during the wet season as well. However, they will have to manage the risks of pollution by overflow in the barges.

As expected, FA1 detects deforestation linked to gold mining all year round (Fig. 11, left), while FA2 detects almost all the disturbance areas during the dry season and only a few during the wet season. This is consistent with the capacity of each sensor.

Fig. 11 (right) shows a much better temporal adequacy/precision of the SAR imagery: 80% of the reference polygons are first detected by FA1, including 40% of more than 3 months of optical delay. The majority of FA2 delays are due to the limitations of optical sensors because of cloud cover, with the delay increasing during the wet season.

Fifty-eight out of the 433 polygons (13%) found first by FA1 and 25 out of the 107 polygons (23%) found first by FA2 may be explained by the timing of the acquisitions of each sensor.

Of the 17 polygons found more than 4 months earlier by FA2, two-

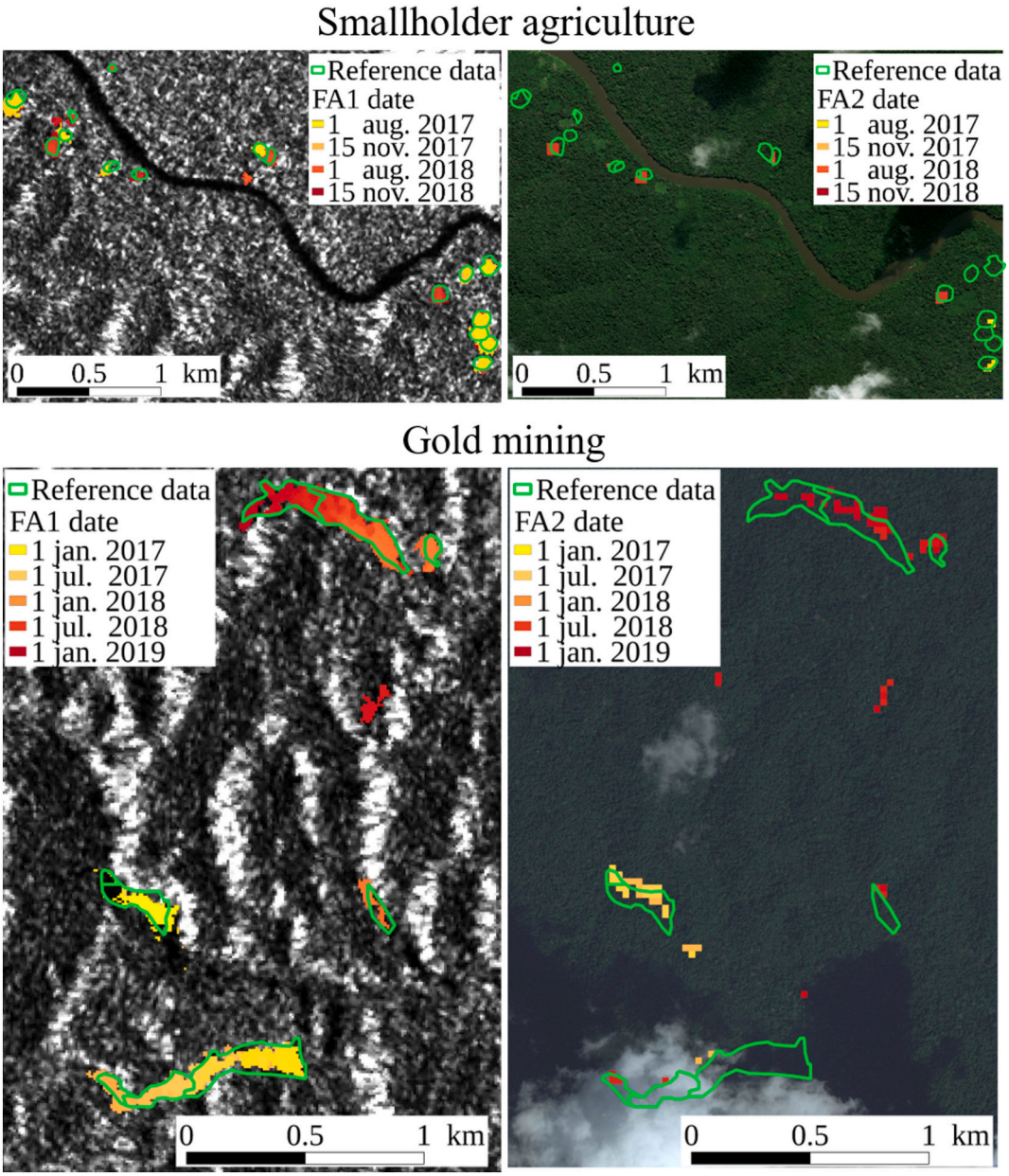

Fig. 6. Spatial comparison of forest loss maps from FA1 (SAR) (left – Background: Sentinel-1 SAR image) and from FA2 (optical) (right – Background: Bing aerial optical image). Reference data are drawn in green. The two upper maps are centered on 3°12 N and 52°25. (For interpretation of the references to colour in this figure legend, the reader is referred to the web version of this article.)

thirds were FA2 commission errors due to close gold mining activities that started before the study period. The other one-third were due to the same phenomenon of overlap seen in smallholder agriculture (Fig. 9) because of the close proximity of multiple new gold mining sites.

These examples show the benefits of SAR imagery over optical imagery in the tropics, especially in a NRT context.

3.4. Annual rate of forest change

Fig. 12 shows the forest disturbance maps for FA1 applied at the country scale in French Guiana between 2016 and 2018. Eight subsets of 8×12 km areas highlight the various sizes and distributions of the disturbed areas.

Agriculture practices are seen in all subsets except in subset 3 and 5. Two spatial patterns are distinguishable: small circular-shaped parcels and a bit biggest square-shaped parcels. This corresponds to the agricultural practices of different communities. Gold mining meandering shape is visible in subsets 2 and 3. Subset 5 shows an area of forest exploitation. We can see the detection of the roads and small patch detected with high density.

Fig. 13 compares the annual rates of forest cover change over French Guiana from FA1, FA2 and the GFW tree cover loss (annual) dataset. The annual rate of change is calculated using the Eq. (4) from Puyravaud (2003) as follows:

$$r = \left(\frac{1}{t2 - t1}\right) \times ln(A2 - A1) \quad (4)$$

where A1 and A2 are the surface areas of the forest in years t1 and t2, respectively. Note that r is negative when the forest lost is greater than the forest gained. FA1 and FA2 both produce FAs in a NRT context, whereas the GFW tree cover loss dataset is an annual product.

FA1 (in green in Fig. 13) shows a decrease in the deforestation rate

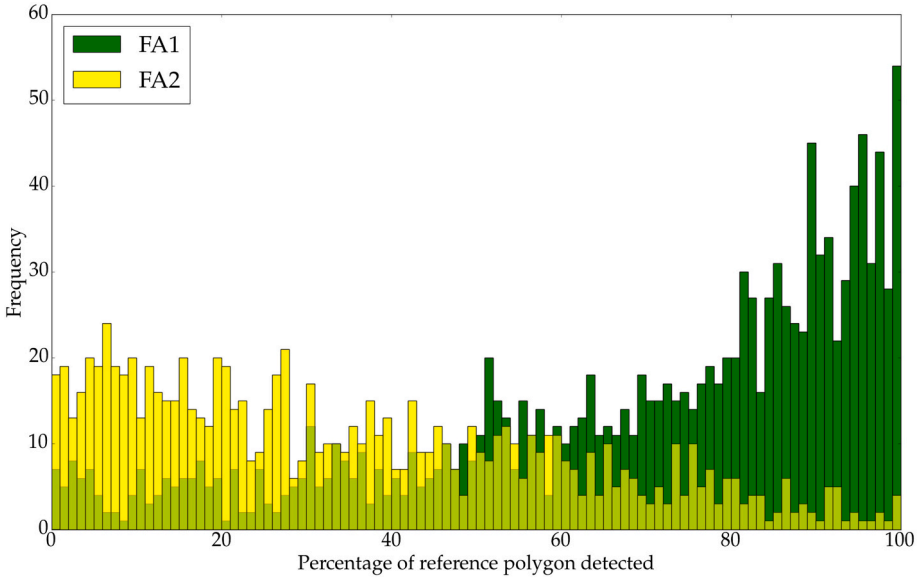

Fig. 7. Histogram of percentage of reference polygons covering by both methods.

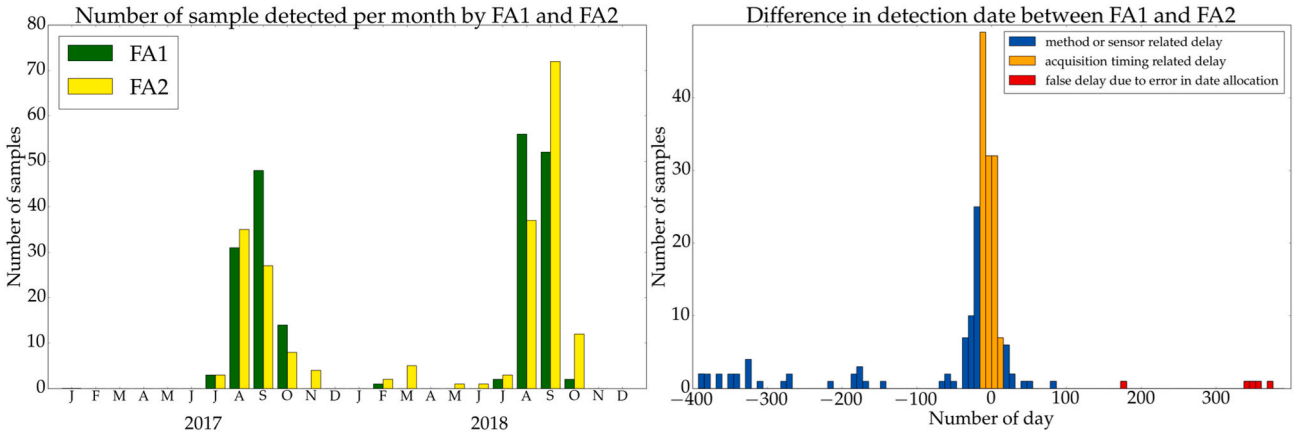

Fig. 8. Regarding smallholder agriculture: number of detected reference samples per month for the FA1 (green) and for the FA2 (yellow) Forest Alerts systems (left), and histogram of the difference in detection date of the reference samples (right), where negative values indicate an earlier detection in the FA1. (For interpretation of the references to colour in this figure legend, the reader is referred to the web version of this article.)

between 2016 (5,619 ha deforested) and 2017 and a stabilization from 2017 (3,169 ha deforested) to 2018 (3,430 ha deforested). The same trends are found in the GFW tree cover loss which aim to quantify the amount of change in one year. As seen in section 3.2, the SAR-based system raised more FAs than the optical-based system, which is attributable to the cloud cover conditions and, to a lesser extent, the higher resolution of Sentinel-1.

This graph shows the consistency of the methods as they are all following the same curve.

Fig. 14 gives the forest loss for different size categories in French Guiana, highlighting the importance of small deforested areas, including those by illegal gold mining and smallholder agriculture. Small patches (<2 ha) contribute to half of the forest loss surface area. This result highlights the need of high resolution forest alerts maps.

4. Discussion

We discuss here the potential of the FA1 dataset for operational use with different use cases.

4.1. Potential users

The operationalization of the proposed methodology could be of interest to various actors such as national actors for the management of protected areas, and the management of agricultural and other productive concessions (land census); non-profit organizations for awareness-raising. For example, FA1 could complement the fight against illegal activities (illegal gold mining and illegal land clearing) in French Guiana because it is exploitable during the whole year, automated and cost-effective. However, to be useful in this case, the forest loss detection needs to be characterized as gold mining.

In a more general framework, for an early detection system to be effective, the forest loss alerts must be complemented by alerts prioritization (Weisse et al., 2017), driver's identification, timely results communication and the use by stakeholder (Finer et al., 2018).

Furthermore, in addition to being an alert product, FA1 can also be used to quantify the amount of change for in-depth reporting or analysis as it shows high accuracies. It can therefore be used by scientists, for example, for the quantification of deforestation and the study of climatic events on tree mortality, at least in ever-cloudy regions.

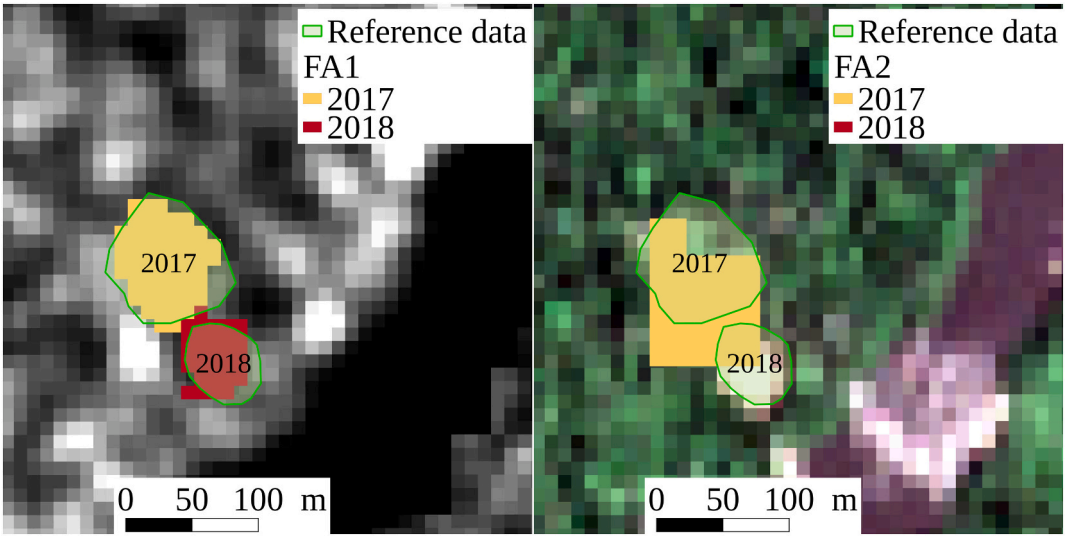

Fig. 9. Reference data are drawn in green and the year of reference is written inside. The 2017 reference parcel is detected by both algorithms in 2017. The 2018 reference parcel is well detected by FA1, although not detected by FA2 and therefore considered as detected in 2017 because of overlapping, creating a false delay of one year of FA1. The maps are centered on 3°16 N and 54°12 W. (For interpretation of the references to colour in this figure legend, the reader is referred to the web version of this article.)

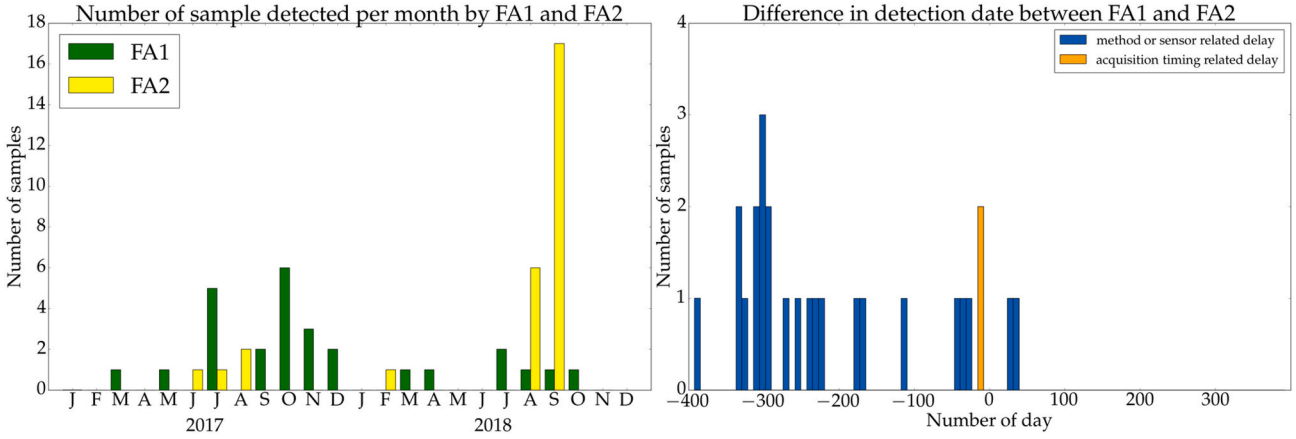

Fig. 10. Regarding forest exploitation: number of detected reference samples per month for FA1 (green) and for FA2 (yellow) Forest Alerts systems (left), and histogram of the difference in detection date of the reference samples (right), where negative values indicate an earlier detection in FA1. (For interpretation of the references to colour in this figure legend, the reader is referred to the web version of this article.)

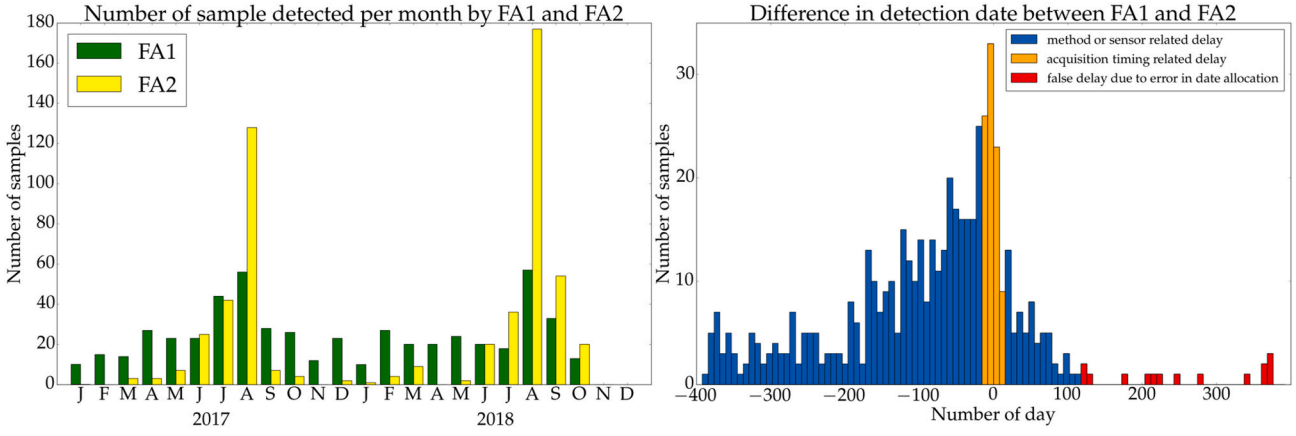

Fig. 11. Regarding gold mining: number of detected reference samples per month for FA1 (green) and for FA2 (yellow) Forest Alerts systems (left), and histogram of the difference in detection date of the reference samples (right), where negative values indicate an earlier detection in FA1. (For interpretation of the references to colour in this figure legend, the reader is referred to the web version of this article.)

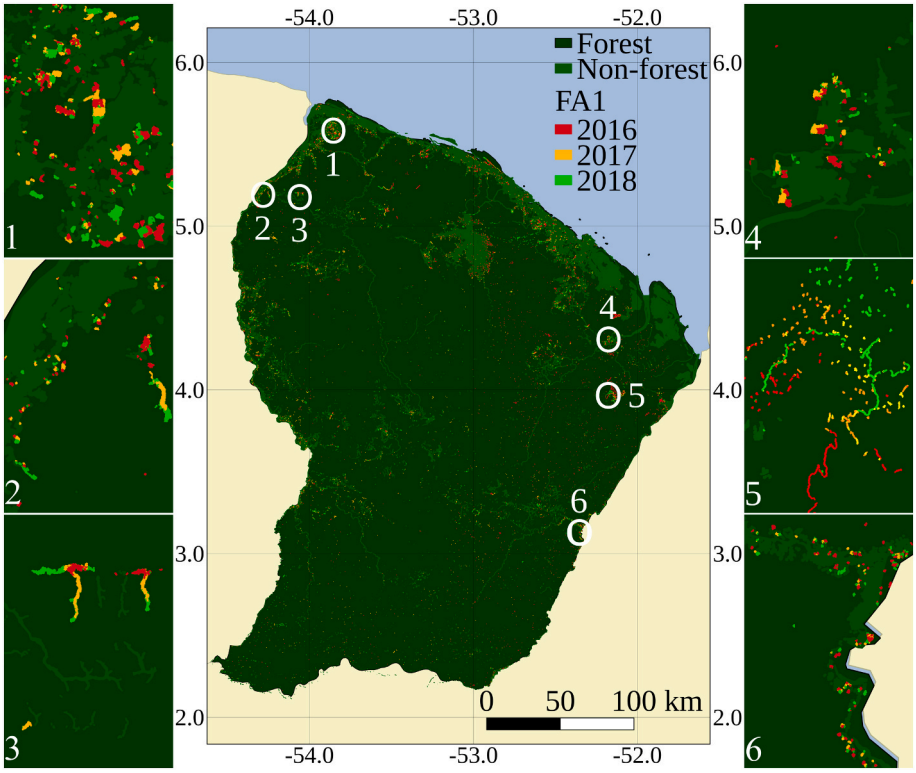

Fig. 12. Forest disturbances over the whole French Guiana from FA1 between 2016 and 2018 at 10-m resolution, and over 8 × 12 km areas in French Guiana, highlighting the various sizes and distributions of disturbed areas.

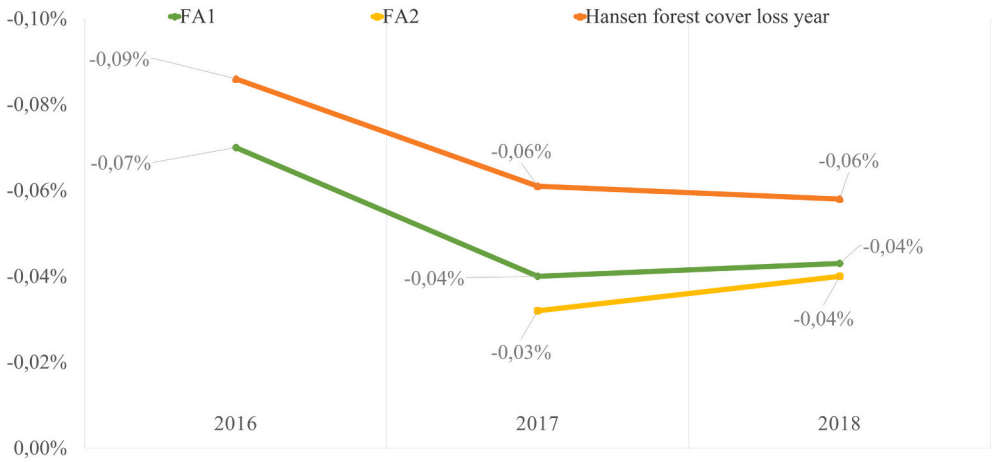

Fig. 13. Rate of change of forest cover on French Guiana, given by various methods. FA1 is in green, FA2 in yellow and Hansen forest cover loss year in orange. (For interpretation of the references to colour in this figure legend, the reader is referred to the web version of this article.)

4.2. Fast alert and detection timing

For illegal or monitored activities, the delay between the disturbance and the detection must be as short as possible. Using a SAR system presents the advantage of guaranteeing the availability of exploitable acquisitions due to their weather-independent capacity. Moreover, the FA1 method is based on a reliable indicator that bypasses environmental effects on SAR signals. Three images are needed to raise an alert with confidence; a deforestation event is therefore confirmed 12 days after its first detection. If the deforestation event is detected in the first Sentinel-1 acquisition after its occurrence, the overall detection delay is between 12 days (deforestation occurring shortly before a Sentinel-1 acquisition) and 18 days (deforestation occurring shortly after a Sentinel-1 acquisition, and 6 days before the first detection in the next Sentinel-1 acquisition). This fast alert timing is particularly useful for illegal forest conversion monitoring (illegal urbanization, illegal gold mining, etc.).

In less urgent cases, accurate deforestation date estimates are also needed, such as in studies related to seasonal deforestation rate. Highly detailed temporal data (as FA1) are currently available except for a few data points collected on the ground.

4.3. Detection confidence

An operational alert system needs low false alarm rates. The FA1 system, with a minimum detected surface area of 0.2 ha, has a mean user

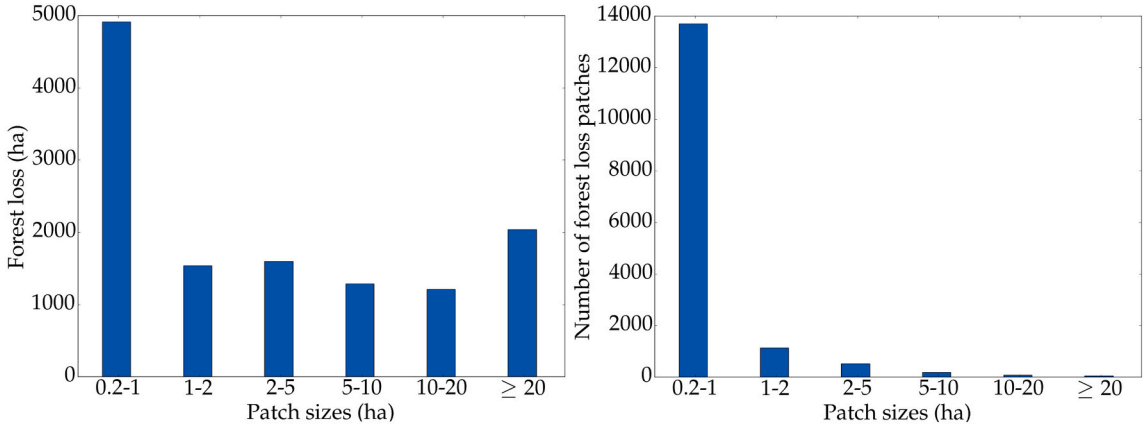

Fig. 14. Number of forest loss patches of different size categories across French Guiana using FA1 (left); Deforested area (ha) of different size categories across French Guiana using FA1 (right).

accuracy of 96% for deforested areas, giving high confidence in the results. The producer's accuracy increases with the MMU, as does the confidence.

Moreover, this system has an 81.5% mean producer's accuracy, giving high confidence to the area estimates, which can be used to account for changes or for target field surveys.

4.4. Production timing

The maximum delay between the acquisitions of 2 Sentinel-1 images over the same orbit is 6 days. An acquired image is available in a maximum of 24 h in the French Product Exploitation Platform for Sentinel (PEPS) and requires less than 1 h to be downloaded, filtered and processed to obtain a deforestation map using the FA1 algorithms. It is therefore possible to provide weekly updates of the FA1 product.

4.5. Scalability

The FA1 method is well adapted to detect French Guiana's types of forest loss. We discuss here its ability to operate on other lands.

Various factors affect the SAR signal and thus forest disturbance detection, including acquisition parameters of the SAR system, environmental factors, type of disturbance and forest characteristics.

Regarding the latter, FA1 was developed for the detection of deforestation in primary tropical forests (high tree height, high canopy density and a low seasonality).

The first condition to see a shadow in the SAR image is to have trees with a sufficient height, as the shadow size is a function of the tree height and the incidence angle of the radar. For example, this particular method will not be efficient for forest heights under 15 m (for flat terrain).

The SAR signal is relatively constant in time in a dense forest with low seasonality. Phenology introduces changes in the SAR signal that are not related to deforestation events. The impact of seasonality on the FA1 method, such as in the dry tropics, has not been studied yet.

Similarly, in a sparse woodland, the SAR signal will also include the soil contribution and its associated variations due to environmental effects. Therefore, the FA1 method applied on a sparse woodland could lead to false alarms.

The disturbance type is another factor affecting Sentinel-1 backscatter. The detection of selective logging will probably not be as accurate as clear-cut and may be characterized by a high density of small detections within the disturbed area. The laws of some countries can also influence the detection of forest loss. For example, Brazilian legislation no longer allows the harvest of several big trees (Brazil nut tree for example). In a deforested area, those remaining trees bring volume scattering of the SAR signal and the decrease of backscatter is not obvious, making the detection more difficult.

FA1 system is also influenced by the number of different SAR looking directions available. In French Guiana, both ascending and descending orbits are available. In regions with a single SAR looking direction, less shadows will appear following a deforestation than when two opposites looking directions are combined.

The FA1 method has been successfully tested in Peru (Bouvet et al., 2018) over a site impacted by smallholder agriculture and agro-industrial development on natural vegetation, comprising mostly evergreen rainforest; and in Gabon over a tropical rainforest impacted by mining activities, palm oil plantation and agricultural activities (Hirschmugl et al., 2020).

Note that the alert product does not distinguish human-induced from natural forest disturbances nor deforestation from forestry and other land use dynamics.

5. Summary and conclusions

Tropical forests are an important carbon sink and high biodiversity locations. Monitoring forest disturbances is a major issue that requires efficient and accurate tools that are available in NRT.

French Guiana's forest is mostly affected by small-scale disturbances occurring year-round partly caused by illegal activities (such as gold mining) and leading to health and environmental issues. The early detection of small-scale disturbances is therefore of environmental and social importance for French Guiana. Existing operational Forest loss Alerts (FA) systems are mostly optical-based and the persistent cloud cover of the region leads to temporal delays, poor detection (with automated method), or high-cost production.

With its dense time series of SAR data independent to cloud cover and its 10-m pixel resolution, Sentinel-1 provides a free efficient tool in this situation.

A FA system in NRT based on the method developed by Bouvet et al. (2018) and using Sentinel-1 SAR data (FA1) was developed and evaluated over French Guiana between 2016 and 2018. Spatial accuracy assessments are based on 1,867 reference data polygons, totaling 2,124.5 ha, collected by French organizations independently from this study, and they described several deforestation practices of the tropics (small/large surface areas, dry/wet season activities, etc.). The SAR FA was compared with an optical FA system (Hansen et al., 2016) (FA2) using free and open data and with a NRT goal in the tropics.

FA1 achieves better results than FA2 in terms of spatial validation on all types of deforestation: the producer's accuracy for FA1 is between 75.9 and 89.4%, whereas that for FA2 is between 31.9 and 40%. The main reason for the poor performance of the optical FA is the very high

cloud cover of the region.

The temporal comparison regarding dry season activities (such as smallholder agriculture) shows no significant difference between the two methods, and half of the delays in each dataset could be explained by the sensor acquisition timing. In contrast, for year-round activities (such as gold mining), the optical-based system has a median temporal delay of 143 days (more than 4.5 months). However, the detection date of the SAR-based dataset shows the same trends as the activity on the ground.

We demonstrate that the use of a SAR-based method is necessary to better identify the deforestation timing. The Sentinel-1 based method produces less omission errors (45.3% on average) than the Landsat method, although the last one produces less commission errors (2.1% on average) and even made no commission errors at all in most validation cases.

It was expected that we could use a combination of SAR and optical data, such as a joint use of Sentinel-1 and Sentinel-2, to enhance the detection performance as shown by (Reiche et al., 2018). However, for the detection of wet season forest disturbance activities, the limited availability of exploitable optical data is not suited to an operational alert system.

We show the annual rate of change from 2016 to 2018 with the two NRT methods FA1 and FA2 and from an annual deforestation product meant to give the annual disturbed surface area: the GFW Tree Cover Loss product. The 3 datasets indicate a decrease in deforestation from 2016 to 2017 and a stabilization in 2018 compared to 2017. Regarding the two NRT datasets, the SAR-based system raised more FAs (+622 ha in 2017 and + 200 ha in 2018) than the optical-based FA system.

Finally, we discuss the ability of FA1 dataset to be a useful operational system. The FA1 map of this study is available in http://cesbio.mass.net/.

CRediT authorship contribution statement

Marie Ballère: Methodology; Software; Validation; Formal analysis; Investigation; Data curation; Writing - original draft; Writing - review & editing; Visualization. **Alexandre Bouvet:** Conceptualization; Methodology; Formal analysis; Writing - original draft; Writing - review & editing. **Stéphane Mermoz:** Conceptualization; Methodology; Formal analysis; Writing - original draft; Writing - review & editing. **Thuy Le Toan:** Conceptualization, Writing - review & editing. **Thierry Koleck:** Software. **Caroline Bedeau:** Resources. **Mathilde André:** Resources. **Elodie Forestier:** Resources. **Pierre-Louis Frison:** Supervision. **Cédric Lardeux:** Resources.

Declaration of Competing Interest

None.

Acknowledgements

Marie Ballère was supported by the Centre National d'Etudes Spatiales (CNES) and the Word Wildlife Fund (WWF) by the research allowance co-financing agreement n° CNES : 3018. The Centre d'Etudes Spatiales de la Biosphère (CESBIO) also participated financially. We thank the Office National des Forêts (ONF), French Guiana, and Etat-Major contre l'Orpaillage et la Pêche Illicites (EMOPI) for the provision of reference data and the Parc Amazonien de Guyane (PAG) for the open availability of their land cover map.

The authors would like to thank Brice Boclet for his advice on the writing and the reviewer for the valuable comments.

References

WWF, 2018. Lutte Contre l'Orpaillage Illégal en Guyane: Orientations Pour une Efficacité Renforcée.

Alvarez-Berríos, N.L., Mitchell Aide, T., 2015. Global demand for gold is another threat for tropical forests. Environ. Res. Lett. 10, 014006 https://doi.org/10.1088/1748-9326/10/1/014006.

Arévalo, P., Olofsson, P., Woodcock, C.E., 2020. Continuous monitoring of land change activities and post-disturbance dynamics from Landsat time series: a test methodology for REDD+ reporting. Remote Sens. Environ. 238, 111051. https://doi.org/10.1016/j.rse.2019.01.013.

Bouvet, A., Mermoz, S., Ballère, M., Koleck, T., Le Toan, T., 2018. Use of the SAR shadowing effect for deforestation detection with Sentinel-1 time series. Remote Sens. 10, 1250. https://doi.org/10.3390/rs10081250.

Bullock, E.L., Woodcock, C.E., Olofsson, P., 2020. Monitoring tropical forest degradation using spectral unmixing and Landsat time series analysis. Remote Sens. Environ. 238, 110968. https://doi.org/10.1016/j.rse.2018.11.011.

Cochran, W., 1977. Sampling Techniques. John Wiley Sons.

Colchester, M., 1997. Guyana: fragile frontier. Race Cl. 38, 33–56. https://doi.org/10.1177/030639689703800403.

De Kom, J.F.M., van der Voet, G.B., de Wolff, F.A., 1998. Mercury exposure of maroon workers in the small scale gold mining in suriname. Environ. Res. 77, 91–97. https://doi.org/10.1006/enrs.1998.3835.

Demaze, M.T., Manusset, S., 2008. L'agriculture itinérante sur brûlis en Guyane française: la fin des durabilités écologique et socioculturelle? Cah. O.-m. 61, 31–48.

Diniz, C.G., de Souza, A.A.A., Santos, D.C., Dias, M.C., da Luz, N.C., de Moraes, D.R.V., Maia, J.S.A., Gomes, A.R., da Narvaes, I.S., Valeriano, D.M., Maurano, L.E.P., Adami, M., 2015. DETER-B: the new Amazon near real-time deforestation detection system. IEEE J. Sel. Top. Appl. Earth Obs. Remote Sens. 8, 3619–3628. https://doi.org/10.1109/JSTARS.2015.2437075.

Eisler, R., 2004. Biogeochemical, Health, and Ecotoxicological Perspectives on Gold and Gold Mining. CRC press.

Finer, M., Novoa, S., Weisse, M.J., Petersen, R., Mascaro, J., Souto, T., Stearns, F., Martinez, R.G., 2018. Combating deforestation: from satellite to intervention. Science 360, 1303–1305. https://doi.org/10.1126/science.aat1203.

Forte, J., 1999. Karikuri: the evolving relationship of the Karinya people of Guyana to gold mining. New west Indian Guid. West-Indische Gids 76, 59–82.

Friedlingstein, P., Jones, M.W., O'Sullivan, M., Andrew, R.M., Hauck, J., Peters, G.P., Peters, W., Pongratz, J., Sitch, S., Le Quéré, C., Bakker, D.C.E., Canadell, J.G., Ciais, P., Jackson, R.B., Anthoni, P., Barbero, L., Bastos, A., Bastrikov, V., Becker, M., Bopp, L., Buitenhuis, E., Chandra, N., Chevallier, F., Chini, L.P., Currie, K.I., Feely, R. A., Gehlen, M., Gilfillan, D., Gkritzalis, T., Goll, D.S., Gruber, N., Gutekunst, S., Harris, I., Haverd, V., Houghton, R.A., Hurtt, G., Ilyina, T., Jain, A.K., Joetzjer, E., Kaplan, J.O., Kato, E., Klein Goldewijk, K., Korsbakken, J.I., Landschützer, P., Lauvset, S.K., Lefèvre, N., Lenton, A., Lienert, S., Lombardozzi, D., Marland, G., McGuire, P.C., Melton, J.R., Metzl, N., Munro, D.R., Nabel, J.E.M.S., Nakaoka, S.-I., Neill, C., Omar, A.M., Ono, T., Peregon, A., Pierrot, D., Poulter, B., Rehder, G., Resplandy, L., Robertson, E., Rödenbeck, C., Séférian, R., Schwinger, J., Smith, N., Tans, P.P., Tian, H., Tilbrook, B., Tubiello, F.N., van der Werf, G.R., Wiltshire, A.J., Zaehle, S., 2019. Global carbon budget 2019. Earth Syst. Sci. Data 11, 1783–1838. https://doi.org/10.5194/essd-11-1783-2019.

Hansen, M.C., Potapov, P.V., Moore, R., Hancher, M., Turubanova, S.A., Tyukavina, A., Thau, D., Stehman, S.V., Goetz, S.J., Loveland, T.R., Kommareddy, A., Egorov, A., Chini, L., Justice, C.O., Townshend, J.R.G., 2013. High-resolution global maps of 21st-century Forest cover change. Science 342, 850–853. https://doi.org/10.1126/science.1244693.

Hansen, M.C., Krylov, A., Tyukavina, A., Potapov, P.V., Turubanova, S., Zutta, B., Ifo, S., Margono, B., Stolle, F., Moore, R., 2016. Humid tropical forest disturbance alerts using Landsat data. Environ. Res. Lett. 11, 034008 https://doi.org/10.1088/1748-9326/11/3/034008.

Hirschmugl, M., Deutscher, J., Sobe, C., Bouvet, A., Mermoz, S., Schardt, M., 2020. Use of SAR and optical time series for tropical Forest disturbance mapping. Remote Sens. 12, 727. https://doi.org/10.3390/rs12040727.

Houghton, R.A., Nassikas, A.A., 2017. Global and regional fluxes of carbon from land use and land cover change 1850-2015: carbon emissions from land use. Glob. Biogeochem. Cycles 31, 456–472. https://doi.org/10.1002/2016GB005546.

Kalamandeen, M., Gloor, E., Mitchard, E., Quincey, D., Ziv, G., Spracklen, D., Spracklen, B., Adami, M., Aragão, L.E.O.C., Galbraith, D., 2018. Pervasive rise of small-scale deforestation in Amazonia. Sci. Rep. 8 https://doi.org/10.1038/s41598-018-19358-2.

Keenan, R.J., Reams, G.A., Achard, F., de Freitas, J.V., Grainger, A., Lindquist, E., 2015. Dynamics of global forest area: results from the FAO global Forest resources assessment 2015. For. Ecol. Manag. 352, 9–20. https://doi.org/10.1016/j.foreco.2015.06.014.

Koleck, T., Ballère, M., Marie-Sainte, W., 2019. S1Tiling, A Multipurpose Open Source Processing Chain for Sentinel-1 Time Series.

Lardeux, C., Kemavo, A., Regeade, M., Rahm, M., Frison, P.-L., Rudant, J.-P., 2019. Mise en oeuvre d'outils open source pour le suivi opérationnel de l'occupation des sols et de la déforestation à partir des données Sentinel radar et optique: études de cas en Guyane et au Togo. Rev. Fr. Photogrammétrie Télédétection 59–70.

Linarès, S., Joubert, P., Gond, V., 2008. Contre l'orpaillage clandestin: la télédétection. Espac. Nat. 32–33.

Office National des Forêts, 2019. Livret de présentation de l'ONF Guyane, ONF Guyane, décembre 2017:http://www1.onf.fr/guyane/++oid++6206/@@display_media.html.

Lohberger, S., Stängel, M., Atwood, E.C., Siegert, F., 2018. Spatial evaluation of Indonesia's 2015 fire-affected area and estimated carbon emissions using Sentinel-1. Glob. Chang. Biol. 24, 644–654. https://doi.org/10.1111/gcb.13841.

Mermoz, S., Le Toan, T., 2016. Forest disturbances and regrowth assessment using ALOS PALSAR data from 2007 to 2010 in Vietnam. Cambodia and Lao PDR. Remote Sens. 8, 217. https://doi.org/10.3390/rs8030217.

Miller, J.R., Lechler, P.J., Bridge, G., 2003. Mercury contamination of alluvial sediments within the Essequibo and Mazaruni River basins, Guyana. Water Air Soil Pollut. 139–166.

Olofsson, P., Foody, G.M., Herold, M., Stehman, S.V., Woodcock, C.E., Wulder, M.A., 2014. Good practices for estimating area and assessing accuracy of land change. Remote Sens. Environ. 148, 42–57. https://doi.org/10.1016/j.rse.2014.02.015.

Olofsson, P., Arévalo, P., Espejo, A.B., Green, C., Lindquist, E., McRoberts, R.E., Sanz, M. J., 2020. Mitigating the effects of omission errors on area and area change estimates. Remote Sens. Environ. 236, 111492. https://doi.org/10.1016/j.rse.2019.111492.

Palmer, C.J., 2002. HIV prevalence in a gold mining camp in the Amazon region. Guyana. Emerg. Infect. Dis. 8, 330–331. https://doi.org/10.3201/eid0803.010261.

Potapov, P., Siddiqui, B.N., Iqbal, Z., Aziz, T., Zzaman, B., Islam, A., Pickens, A., Talero, Y., Tyukavina, A., Turubanova, S., Hansen, M.C., 2017. Comprehensive monitoring of Bangladesh tree cover inside and outside of forests, 2000–2014. Environ. Res. Lett. 12, 104015. https://doi.org/10.1088/1748-9326/aa84bb.

Puyravaud, J.-P., 2003. Standardizing the calculation of the annual rate of deforestation. For. Ecol. Manag. 593–596.

Quegan, S., Yu, Jiong Jiong, 2001. Filtering of multichannel SAR images. IEEE Trans. Geosci. Remote Sens. 39, 2373–2379. https://doi.org/10.1109/36.964973.

Rahm, M., Lardeux, C., 2019. Suivi Quasi Temps Réel de la Déforestation à Partir D'imagerie Radar Sentinel-1: Rapport Final.

Rahm, M., Thibault, P., Shapiro, A., Smartt, T., Paloeng, C., Crabbe, S., Farias, P., Carvalho, R., Joubert, P., 2017. Monitoring the Impact of Gold Mining on the Forest Cover and Freshwater in the Guiana Shield.

Reiche, J., Lucas, R., Mitchell, A.L., Verbesselt, J., Hoekman, D.H., Haarpaintner, J., Kellndorfer, J.M., Rosenqvist, A., Lehmann, E.A., Woodcock, C.E., Seifert, F.M., Herold, M., 2016. Combining satellite data for better tropical forest monitoring. Nat. Clim. Chang. 6, 120–122. https://doi.org/10.1038/nclimate2919.

Reiche, J., Hamunyela, E., Verbesselt, J., Hoekman, D., Herold, M., 2018. Improving near-real time deforestation monitoring in tropical dry forests by combining dense Sentinel-1 time series with Landsat and ALOS-2 PALSAR-2. Remote Sens. Environ. 204, 147–161. https://doi.org/10.1016/j.rse.2017.10.034.

Reymondin, L., Jarvis, A., Perez-Uribe, A., Touval, J., Argote, K., Coca, A., Rebetez, J., Guevara, E., Mulligan, M., 2012. Terra-I: A Methodology for near Real-Time Monitoring of Habitat Change at Continental Scales Using MODIS-NDVI and TRMM.

Tanase, M.A., Aponte, C., Mermoz, S., Bouvet, A., Le Toan, T., Heurich, M., 2018. Detection of windthrows and insect outbreaks by L-band SAR: a case study in the Bavarian Forest National Park. Remote Sens. Environ. 209, 700–711. https://doi.org/10.1016/j.rse.2018.03.009.

Tyukavina, A., Stehman, S.V., Potapov, P.V., Turubanova, S.A., Baccini, A., Goetz, S.J., Laporte, N.T., Houghton, R.A., Hansen, M.C., 2013. National-scale estimation of gross forest aboveground carbon loss: a case study of the Democratic Republic of the Congo. Environ. Res. Lett. 8, 044039 https://doi.org/10.1088/1748-9326/8/4/044039.

Valeriano, D.M., Mello, E.M., Moreira, J.C., Shimabukuro, Y.E., Duarte, V., de Souza, I. M., dos Santos, J.R., Barbosa, C.C.F., de Souza, R.C.M., 2004. Monitoring tropical forest from space: the PRODES digital project. Int. Arch. Photogramm. Remote. Sens. Spat. Inf. Sci. 272–274.

Watanabe, M., Koyama, C., Hayashi, M., Kaneko, Y., Shimada, M., 2017. Development of early-stage deforestation detection algorithm (advanced) with PALSAR-2/ScanSAR for JICA-JAXA program (JJ-FAST). IEEE 2446–2449. https://doi.org/10.1109/IGARSS.2017.8127487.

Weisse, M.J., Petersen, R., Sargent, S., Gibbes, S., 2017. Places to Watch: Identifying High-Priority Forest Disturbance from near-Real Time Satellite Data.

Wheeler, D., Hammer, D., Kraft, R., Steelr, A., 2014. Satellite-Based Forest Clearing Detection in the Brazilian Amazon: FORMA, DETER, and PRODES.

Whittle, M., Quegan, S., Uryu, Y., Stüewe, M., Yulianto, K., 2012. Detection of tropical deforestation using ALOS-PALSAR: a Sumatran case study. Remote Sens. Environ. 124, 83–98. https://doi.org/10.1016/j.rse.2012.04.027.